Supplementary Material

Deamidation of the human eye lens protein γS-crystallin accelerates oxidative aging

Brenna Norton-Baker[1,2], Pedram Mehrabi[2,3], Ashley O. Kwok[1], Kyle W. Roskamp[1], Megan A. Rocha[1],

Marc A. Sprague-Piercy[4], David von Stetten[5], R.J. Dwayne Miller[6], Rachel W. Martin[1,4]*

[1] Department of Chemistry, University of California, Irvine 92697-2025, United States
[2] Department for Atomically Resolved Dynamics, Max-Planck-Institute for Structure and Dynamics of Matter, Luruper Chaussee 149, 22761 Hamburg, Germany
[3] Institute for Nanostructure and Solid-State Physics, Universität Hamburg, HARBOR, Luruper Chaussee 149, 22761 Hamburg, Germany
[4] Department of Molecular Biology and Biochemistry, University of California, Irvine 92697-3900, United States
[5] European Molecular Biology Laboratory, Hamburg Unit c/o Deutsches Elektronen-Synchrotron, Hamburg, Germany
[6] Departments of Chemistry and Physics, University of Toronto, 80 St. George Street, Toronto, Ontario, M5S 3H6, Canada

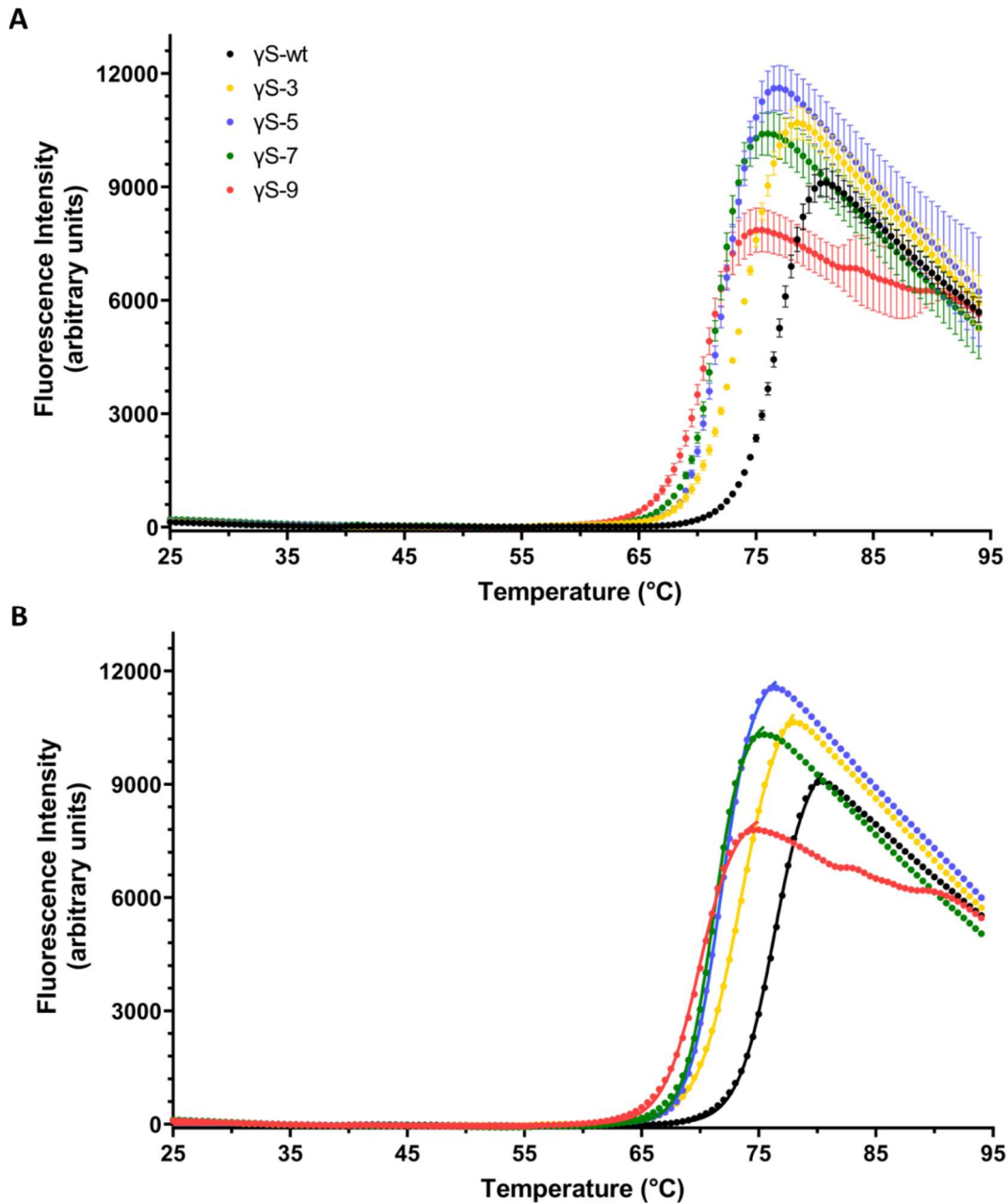*to whom correspondence should be addressed:

rwmartin@uci.edu

Figure S1, related to Figure 2. (A) The average fluorescence intensity from three replicates measured by differential scanning fluorimetry (DSF) for γS-crystallin wild-type (γS-wt, black), 3-site (γS-3, yellow), 5-site (γS-5, blue), 7-site (γS-7, green), and 9-site deamidation variants (γS-9, pink). Data are represented as mean ± SD. (B) The average fluorescence intensity for each protein with overlaid solid lines showing the Boltzmann fit curves calculated for each data set. Only the region of the DSF data up to the fluorescence maxima are used for the Boltzmann fit.
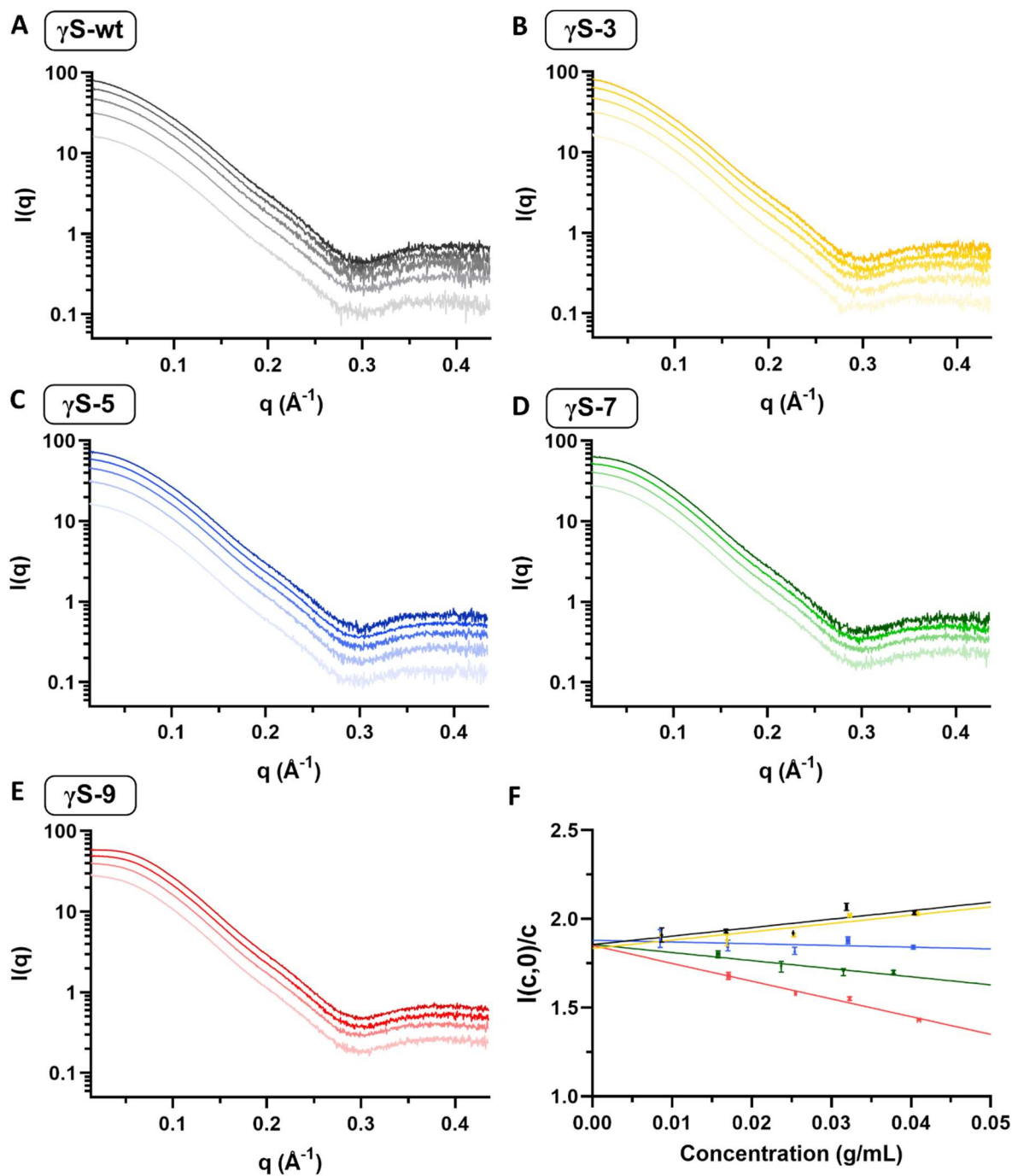
Figure S2, related to Figure 3. SAXS profiles for (A) γS-wt, (B) γS-3. (C) γS-5, (D) γS-7, and (E) γS-9 with concentrations ranging from approximately 40 mg/mL down to either 16 mg/mL (γS-7 and γS-9) or 8 mg/mL (γS-wt, γS-3, and γS-5). Each concentration series was measured in triplicate. (F) The intensity at zero angle over concentration as a function of concentration. Measurements were performed in triplicate. Data are represented as mean ± SD. The y-intercept of the linear regression gives the intensity at zero angle extrapolated to zero concentration.
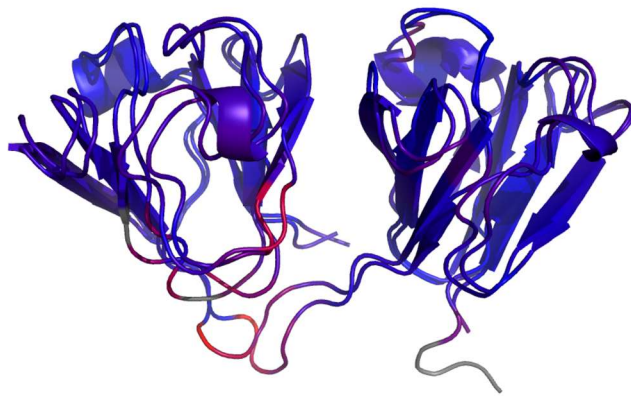
Figure S3, related to Figure 4. Structure alignment of the previously reported NMR structure of γS-wt (PDB: 2M3T) and the novel crystal structure reported here (PDB:7N36). The script *colorbyrmsd* in Pymol was used to highlight areas of minimum pairwise RMSD in blue and maximum in red. The loop containing K154 and K155 as well as the linker region between domains show the maximum difference.
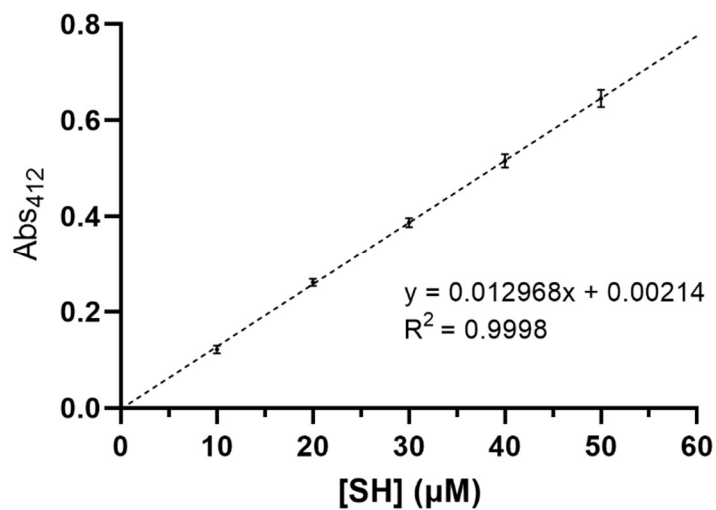
$$y = 0.012968x + 0.00214$$
$$R^2 = 0.9998$$

Figure S4, related to STAR Methods. Calibration curve for Ellman's assay in 2% SDS, 100 mM TRIS pH 8.0 using dithiothreitol (DTT). Measurements were performed in triplicate. Data are represented as mean ± SD. The concentration of thiol is 2× the concentration of DTT. The extinction coefficient calculated is 12968 $M^{-1}cm^{-1}$.
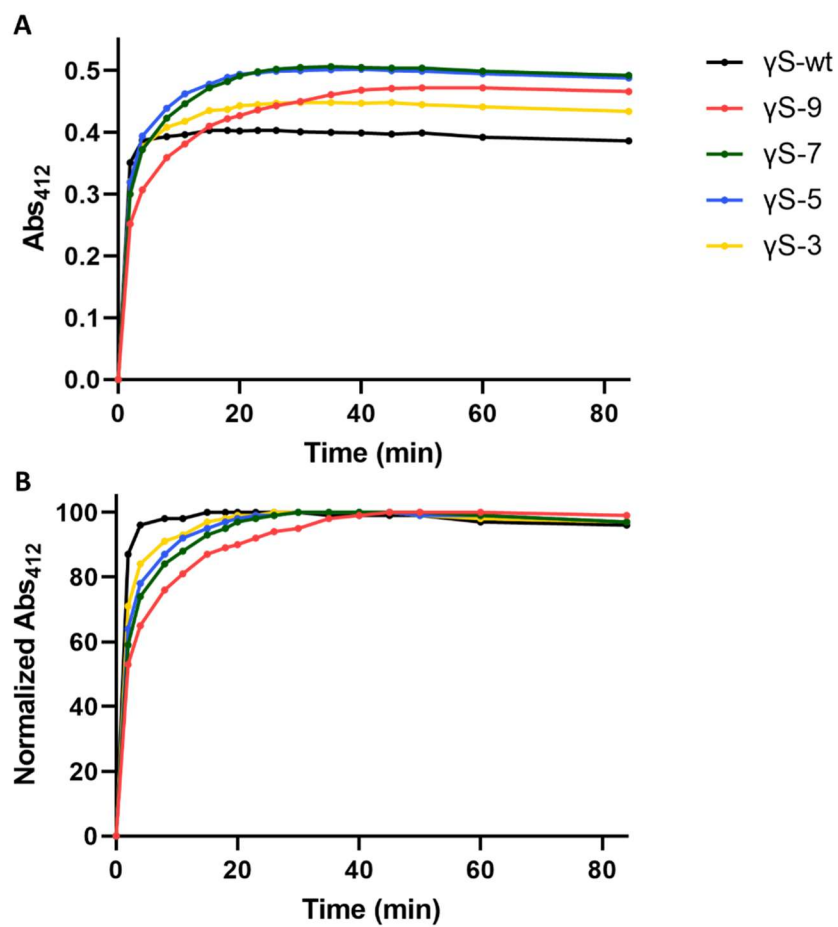
Figure S5, related to Figure 5. (A) Absorbance at 412 nm after the addition of DTNB for γS-wt and each variant. (B) Normalized absorbance at 412 nm for each reaction. Increasing number of deamidated sites leads to longer reaction times to maximum Abs_{412}.
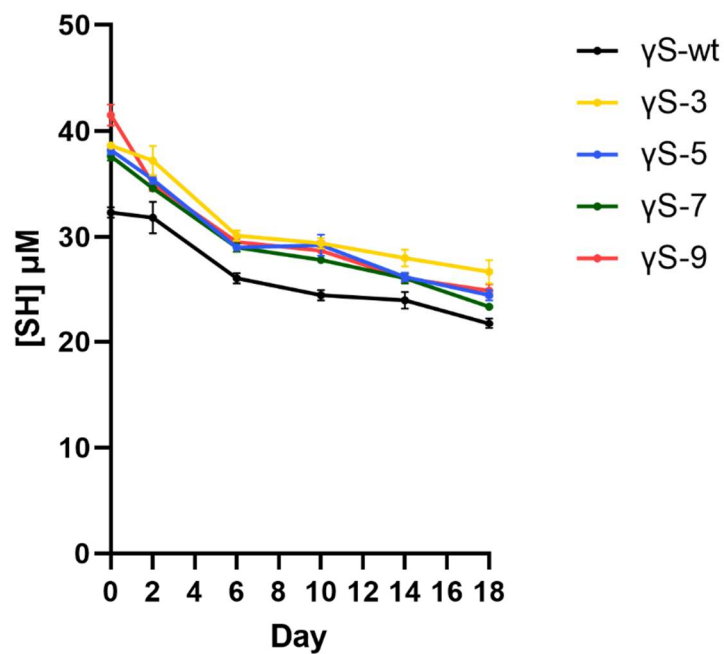
Figure S6, related to Figure 5. (A) Assessment of free thiol concentration over time using Ellman's assay for γS-crystallin wild-type (γS-wt, black), 3-site (γS-3, yellow), 5-site (γS-5, blue), 7-site (γS-7, green), and 9-site deamidation variant (γS-9, pink). Measurements were performed in triplicate. Data are represented as mean ± SD. Proteins were aged at 210 – 250 µM which was diluted 40-fold for these measurements.
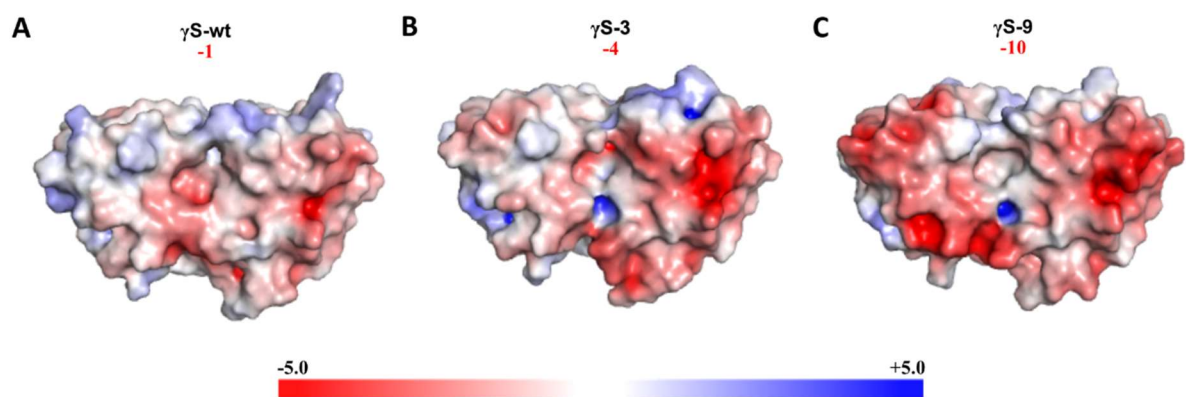
Figure S7, related to Figure 4. Adaptive Poisson-Boltzmann Solver (APBS) electrostatics calculation was used to generate surface charge maps in PyMol for (A) γS-wt PDB:7N36, (B) γS-3 PDB:7N37, and (C) γS-9B PDB:7N3B showing regions of high negative charge with increasing deamidation.

Codon-optimized γS-wt sequence with NcoI and XhoI restriction sites:

```
CCATGGGACATCACCATCACCATCACGAAAATCTTTATTTTCAAGGCAGCAAAACGGGCACCAAAATCACGTTC
TACGAAGACAAAAATTTCCAAGGTCGCCGTTACGACTGTGACTGCGACTGTGCGGACTTCCACACATACCTGTC
CCGTTGCAACTCTATCAAAGTTGAAGGCGGCACCTGGGCTGTATACGAACGCCCGAACTTCGCTGGCTACATGT
ACATCCTTCCGCAGGGCGAATACCCGGAATACCAGCGCTGGATGGGTCTGAACGACCGTCTGTCGTCTTGCCGC
GCTGTACATCTGCCGTCCGGCGGTCAGTACAAAATCCAGATCTTCGAAAAAGGCGACTTCTCCGGCCAGATGTA
CGAAACCACCGAAGACTGCCCGTCTATCATGGAACAATTCCACATGCGCGAAATCCACTCTTGTAAAGTTCTGG
AAGGCGTATGGATCTTCTACGAACTGCCGAACTACCGCGGTCGCCAGTACCTGCTGGACAAAAAGAATACCGC
AAACCGATCGACTGGGGCGCGGCCTCTCCGGCTGTACAGAGCTTCCGTCGTATCGTTGAATAATAACTCGAG
```

Table S1, related to STAR Methods. Oligonucleotides for PCR mutagenesis. A mistranslation of Y11 was identified in the deamidated variants and was corrected by the application of primers *codonY11_fwd* to γS-3 and γS-5 and *codonY11_fwd_2* to γS-7 and γS-9 with *codonY11_rev* used for all deamidated variants.

Primer	Sequence (5' to 3')
N15_fwd	GAC AAA GAT TTC CAA GGT CGC
N15_rev	GCG ACC TTG GAA ATC TTT GTC
Q121_fwd	ATC ATG GAA GAA TTC CAC ATG
Q121_rev	CAT GTG GAA TTC TTC CAT GAT
N144_fwd	TAC GAA CTG CCG GAC TAC
N144_rev	GTA GTC CGG CAG TTC GTA
N54D_fwd	CCG GAC TTC GCT GGC TAC ATG TAC ATC CTT CCG
N54D_rev	GCG TTC GTA TAC AGC CCA GGT GCC GCC TTC
Q93E_fwd	CGT CCG GCG GTG AGT ACA AAA TCC AGA TCT TCG AAA AAG GCG
Q93E_rev	GCA GAT GTA CAG CGC GGC AAG ACG ACA GAC GG
Q64E_fwd	CTT CCG GAG GGC GAA TAC CCG GAA TAC CAG C
Q64E_rev	GAT GTA CAT GTA GCC AGC GAA GTC CGG GCG TTC GTA TAC
Q17E_fwd	GAA GAC AAA GAT TTC GAA GGT CGC CGT TAC GAC TGT GAC TG
Q17E_rev	GTA GAA CGT GAT TTT GGT GCC CGT TTT GCT GCC TTG
Q107E_fwd	GGC GAG ATG TAC GAA ACC ACC GAA GAC TGC CCG TCT ATC
Q107E_rev	GGA GAA GTC GCC TTT TTC GAA GAT CTG GAT TTT GTA CTC ACC GCC G
Q71E_fwd	GGA ATA CGA GCG CTG GAT GGG TCT GAA CGA CCG TCT GTC G
Q71E_rev	GGG TAT TCG CCC TCC GGA AGG ATG TAC ATG TAG CCA GCG
codonY11_fwd	CAA AGA CTT CCA AGG TCG CCG TTA C
codonY11_fwd_2	CAA AGA CTT CGA AGG TCG CCG TTA C
codonY11_rev	TCT TCA TAG AAC GTG ATT TTG GTG CC